Numerical investigation of premixed flames stabilized in a narrow duct with a wall temperature gradient

G.P. Gauthier, G.M.G. Watson, and J.M. Bergthorson
Department of Mechanical Engineering, McGill University
817 Sherbrooke West, Montreal, QC, Canada, H3A 2K6

1 Introduction

Energy production systems involving flames in narrow channels offer many advantages in terms of combustion and thermodynamic properties. The enhanced wall/fluid heat transfer taking place in small ducts provides a way to harvest and promote the heat released by a flame. When the flame thickness is of the same order as the tube diameter [1], the flame structure is significantly influenced by hydrodynamic effects which are in turn tightly coupled to thermo-diffusive effects. Hence, the flame profile not only varies axially along the tube length, but also varies radially. This radial dependence is typically not considered in the investigation of flames inside tubes, as one-dimensional models are generally used. These models are considered to provide an effective means of predicting qualitative flame behaviors. However, the relative importance of two-dimensional effects on these predictions is yet to be assessed. The aim of this study is to include the two-dimensional effects in the modeling of a flame stabilized in a narrow duct with a wall temperature gradient. The variation of mixture composition is used to evaluate the leading order effects influencing the flame behavior. Results are compared to those obtained from a one-dimensional model to further evaluate the relative importance of two-dimensional effects.

2 Model and Case Description

In this work, the axisymmetric case of a premixed methane flame stabilized in a 2 mm diameter tube subjected to a linearly increasing wall temperature is investigated. The wall temperature distribution allows the flame to stabilize at a location where the temperature dependent burning rate matches the specified incoming mass flow rate. The two-dimensional Navier-Stokes equations with detailed chemistry are solved for different mixture compositions.

In order to solve the Navier-Stokes equations for compressible reacting flow, a finite volume formulation is employed. It is based on the mathematical formulation for low-Mach number reacting flows. Neglecting the Soret and Dufour effects, the governing conservation equations for mass, species, momentum, and energy at steady state can be written in the cartesian form as follows:

$$\nabla \cdot (\rho \vec{U}) = 0 \tag{1}$$

Correspondence to: jeff.bergthorson@mcgill.ca

$$\rho\vec{U}\cdot\nabla Y_i - \nabla\cdot(\rho D_i\nabla Y_i) = \dot{\omega}_i \tag{2}$$

$$\rho\left(u\frac{\partial u}{\partial x}+v\frac{\partial u}{\partial y}\right) = -\frac{\partial p}{\partial x}+\frac{\partial}{\partial x}\left\{\mu\left[2\frac{\partial u}{\partial x}-\frac{2}{3}\left(\frac{\partial u}{\partial x}+\frac{\partial v}{\partial y}\right)\right]\right\}+\frac{\partial}{\partial y}\left\{\mu\left(\frac{\partial u}{\partial x}+\frac{\partial v}{\partial y}\right)\right\} \tag{3}$$

$$\rho\vec{U}\cdot\nabla h - \nabla\cdot(\rho\alpha\nabla h) = 0 \tag{4}$$

$$h=\sum_{i=1}^{N}Y_i h_i \qquad\qquad h_i = h_i^{\circ}+\int_{T_0}^{T}c_{p_i}dT \tag{5}$$

In Equation (2), D_i is the mixture averaged diffusion coefficient and $\dot{\omega}_i$ is the net production rate of species i. Equation (3) shows the conservation of momentum in the *x*-direction. The *y*-direction equation is not shown as its formulation is similar. The momentum equation is appropriately formulated in order to use a SIMPLE (Semi-Implicit Method for Pressure Linked Equations) algorithm [7] that iteratively marches towards the steady-state solution. In Equation (4), the heat generated by the chemical reactions is included in the h term as it comprises the enthalpies of formation as shown in Equation (5). The inter-species diffusion term in the energy equation is not included as its effect is assumed to be negligible.

Detailed chemistry is handled using an operator-split method [6] that calculates a reaction rate based upon an Arrhenius kinetics integration over the residence time in each cell. The reaction mechanism is chosen to be DRM19, a reduced version of GRI-Mech 1.2 that includes 19 species and 84 chemical reactions [8].

The main test case comprises a 2.85 cm long tube of 2 mm diameter. The wall temperature increases linearly from 800 K to 1800 K over a distance of 2.25 cm as shown in Fig. 1 by a black solid line. Uniform wall temperature sections are specified at the inlet and outlet to minimize the influence of their respective boundary conditions. The fluid inlet conditions are specified as fixed values and Neumann boundary conditions are set at the outlet. In addition, there is no slip at the wall and the wall temperature is specified.

Different mixture compositions are chosen for this study, as shown in Table 1. Mixtures *A, B, C* are methane-air mixtures at equivalence ratios of 1, 0.7, and 1.4 respectively. Adiabatic flame speeds of these mixtures for an inlet temperature of 300 K are computed using the reaction mechanism mentioned above. Adiabatic flame speed is considered to have a leading order effect on the flame position. Indeed, this flame property provides a mean of inter-relating changes in heat release, reaction rates, diffusivity, etc. that depend on mixture composition. However, this relationship is provided in the absence of heat loss and curvature/stretch effects which are significant in the case of a flame stabilized inside a tube. In order to assess the relative importance of these effects, mixtures *D, E, F, G* are tuned to match the adiabatic flame speeds of the methane-air mixtures (*A, B, C*) by varying the level of nitrogen dilution. All simulations are performed using the same inlet velocity of 2.667 m/s at 800 K which allows a comparison of the results based on flame position.

To obtain accurate two-dimensional results, special precautions are taken to ensure sufficient grid refinement in the flame. A special grid refinement procedure is performed that progressively refines the grid in the flame region up to a level where a grid independent flame location is obtained. This level is reached for cell sizes of the order of 10 μm. Sufficient computational power was provided by the Compute Canada cluster resources that allow the use of parallel processing capabilities. Each simulation required the use of 16 processors for around 200 hours in order to reach the refined converged solution.

Mixtures	ϕ	$N_2\%$ air	T_{ad} (K)	S_L (m/s)	δ_f (mm)
A	1	79	2224	0.393	0.412
B	0.7	79	1843	0.206	0.601
C	1.4	79	2001	0.142	0.943
D	1	83.2	1977	0.206	0.655
E	1	84.9	1860	0.142	0.866
F	0.7	74.2	2087	0.393	0.379
G	1.4	72.6	2274	0.393	0.422

Table 1: Composition of different mixtures is shown with their respective adiabatic temperatures, flame speeds, and flame thicknesses calculated at $T_i = 300\,K$. Level of nitrogen dilution is used to match the adiabatic flame speeds over different equivalence ratios.

3 Results and Discussion

Two-dimensional results were obtained with an inlet velocity of 2.667 m/s for all the different mixture cases. Figure 1 shows the temperature profiles along the longitudinal direction obtained with the stoichiometric mixture *A*, at different values of radial distance. The trends in temperature profiles are similar for all mixtures. A first section is located upstream of the flame where the wall temperature is higher than the fluid temperature. It is followed by the flame section where the fluid temperature, due to reaction, becomes higher than the wall temperature and then cools down. Heat is thus drawned from the fluid to the wall. Close to the outlet, a second wall heating section takes place. In Fig.1, the two-dimensional nature of temperature profiles is observed, as shown by the difference between fluid temperatures at the wall and at the center-line. It can be seen that wall thermal effects are of reduced importance at the center-line, which explains that the peak flame temperature is observed in the middle of the channel, away from the heat loss interface. Note that hydrodynamics effects also play a role in this radial temperature dependence, as larger mass flux of reactants is conveyed in the middle due to the no-slip condition at the wall, which intensifies the heat production at the center-line. Hence, two-dimensional effects are shown to have a strong effect on the radial temperature distribution.

It is of interest to compare the flame structure for different equivalence ratios. Heat release profiles provide a relevant assessment of flame structure as is it based on the net contribution from all individual species. Figure 2 shows different heat release profiles over a radial cross-section of the duct. Equivalence ratios of 0.7 (mixture *B*), 1 (mixture *A*), and 1.4 (mixture *C*) are considered. It can be seen that flame axial positions are ordered in the same way as the respective laminar flame speeds. Yet, the lean and stoichiometric mixtures lie very close to one another, whereas the rich mixture lies much further downstream. In order to explain these trends, it is of interest to consider flame parameters such as thickness and flame surface area. It can be qualitatively observed that the rich flame has a thicker structure than the two other ones, which agrees with the adiabatic flame results shown in Table 1. This increased thickness broadens the section over which wall heat loss affects the flame, which hinders the burning rate, which in turn pushes the flame downstream. For this rich mixture, a stronger wall heat loss might explain why the peak heat release distribution is more concentrated in the middle of the channel, away from the wall. On the other hand, lean and stoichiometric flames show similar thicknesses; however, the lean mixture demonstrates a larger curvature which makes the flame area larger. This promotes the burning rate, which might explain why the lean flame sits so close to the stoichiometric flame, even if their laminar flame speeds differ significantly. Hence, the respective contributions of two-dimensional effects to flame position related to wall heat loss and to flame curvature/stretch are shown to vary based on the mixture composition. This explains why the respective differences in laminar flame speeds are not proportionally reflected in the flame position results.

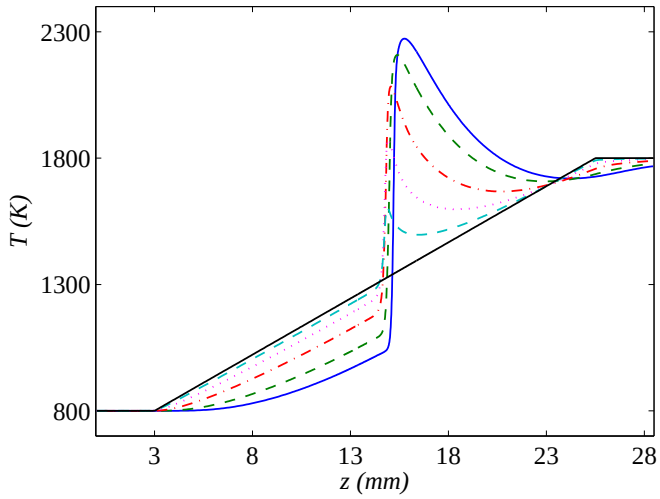

Figure 1: Distribution of temperature over the tube length for a stochiometric methane-air flame (mixture *A*) at different radial positions: *r*=0 (solid blue line), *r*=0.42 mm (dashed green line), *r*=0.68 mm (dash-dot red line), *r*=0.84 mm (dotted purple line), *r*=0.94 mm (dashed cyan line), *r*=1.0 mm (solid black line).

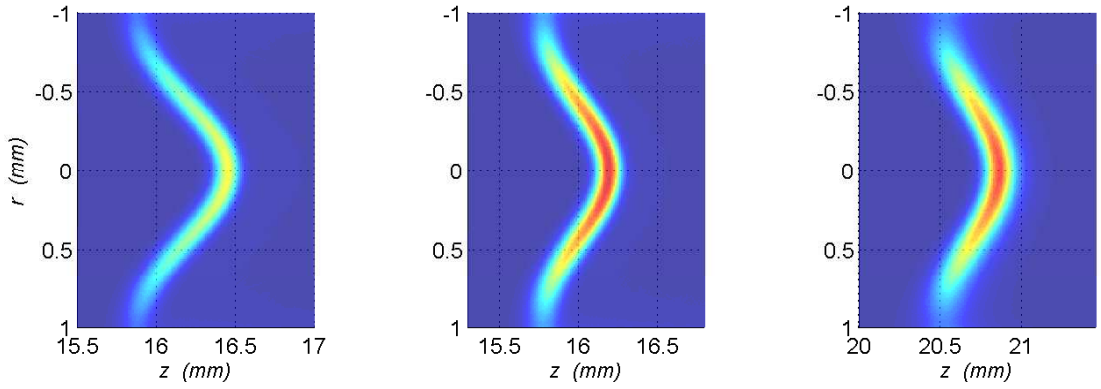

Figure 2: Heat release profiles for methane-air flames at different equivalence ratios. A lean case ($\phi = 0.7$) is shown on the left (mixture *B*), a stoichiometric case is shown in the middle (mixture *A*), a rich case ($\phi = 1.4$) is shown on the right (mixture *C*). Color mapping ranges between 0 and $20 MW/m^3$ and is the same for each case.

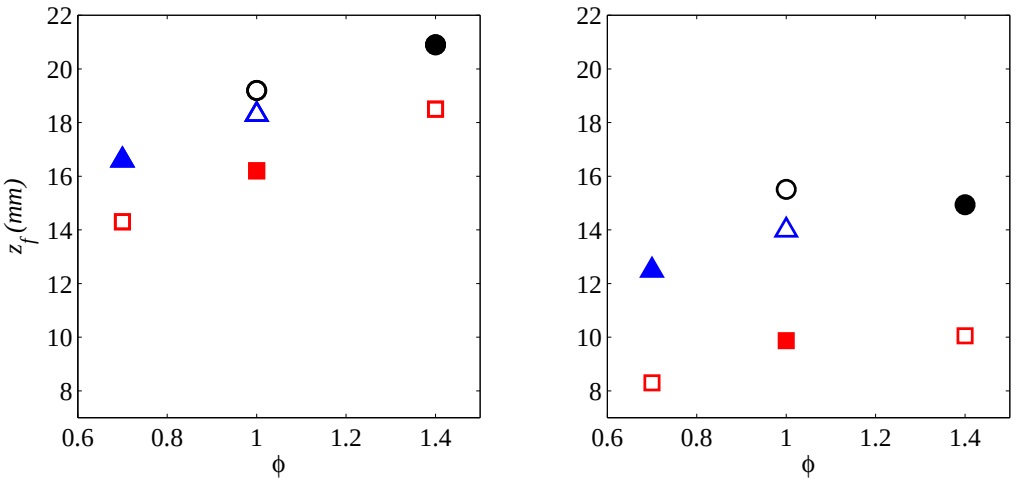

Figure 3: Results for flame position as a function of equivalence ratio for the two-dimensional model (left), and the constant Nu model (right). Mixtures with regular air dilution (filled markers), and tuned dilution levels (empty markers), correspond to those in Table 1. Sets of points having the same laminar flame speed have the same shape.

To obtain of fundamental understanding of flames stabilized inside narrow channels, it is of interest to identify the leading order effects influencing flame position. The flame stabilizes at a location where the flame propagation velocity matches the incoming flow velocity. Hence, laminar flame speed is considered to be of leading importance when predicting this position. As mentioned above, other effects should be included to capture the important physics of the system. Typically, one-dimensional models not only take into account laminar flame properties of a mixture, they also take into account, in a simplified manner, the effect of heat loss on these flames. In these models, the radial heat transfer with the wall is accounted for by specifying the convective heat transfer coefficient or Nusselt number inside the energy equation [2] [3] [4] [5]. Nonetheless, the flame is still considered as uniform in the radial direction, which neglects curvature effects. For this analysis, the same mixtures subjected to the same conditions are modeled using a one-dimensional model that uses a constant Nusselt number approximation [4].

Figure 3 shows the respective flame positions for all mixtures, for both the two-dimensional model and the constant Nu model. By looking first at the two-dimensional results for flame positions, it can be seen that respective positions follow the same ordering as laminar flame speeds. This suggests that laminar flame speed is of primary importance in predicting flame position. When comparing results from two different models, flame positions are shown to be underestimated by a significant amount, which underlines the limited quantitative accuracy of the constant Nusselt number model predictions. Trends in relative positions are similar, except for the rich methane-air flames. This suggests that the inclusion of heat loss in the modeling effort is of importance in capturing the dominant physics of the system. However, the qualitative predictions of the constant Nu model present flaws in the case of the rich methane-air mixtures (*C* and *G*) as their relative flame positions are under-predicted. It was previously discussed that rich flames demonstrate a significant radial variation in heat release. This suggests that the two-dimensional effects that are not considered in the one-dimensional model can significantly influence the system at certain conditions, such as in the rich methane-air case.

4 Conclusion

In this work, two-dimensional simulations of premixed methane flames stabilized in a 2 mm diameter duct subjected to a specified wall temperature distribution are performed. The two-dimensional nature of these flames is investigated. The variation of mixture composition is used to evaluate the leading order effects influencing the flame behavior. Different mixture compositions having equal laminar flame speeds are compared to determine the relative importance of laminar flame speed on flame position. To evaluate the relative importance of two-dimensional effects, results obtained from a one-dimensional model that includes a constant Nusselt number assumption are compared to the two-dimensional results.

It is found that flames in tubes exhibit a structure that is two-dimensional. Structure properties such as flame curvature and flame thickness are qualitatively observed to vary based on mixture composition. Laminar flame speed is shown to be of leading importance in predicting the flame position. The consideration of heat transfer with the wall further improved the prediction of trends in flame position as it is demonstrated with the one-dimensional model results. However, other two-dimensional effects can significantly influence the physics of the system, as demonstrated by the relative inaccuracy of the constant Nusselt Number model in the case of the rich methane-air mixtures. It was also shown that the one-dimensional model does not provide quantitatively accurate results, as flame positions are significantly underpredicted.

5 Acknowledgements

This work was funded by the Fonds Québecois de la Recherche sur la Nature et les Technologies (FQRNT). We also thank the Consortium Laval, Université du Québec, McGill and Eastern Quebec (CLUMEQ) for providing resources for the computations.

References

[1] Daou J., Matalon M. (2002). Influence of Conductive Heat-Losses on the Propagation of Premixed Flames in Channels. Combustion and Flame 128: 321-339

[2] Yu Y., Choi C.W. (2003). An analysis of sub-limit flame dynamics using opposite propagating flames in mesoscale channels. Combustion and Flame 133: 483-493

[3] Ronney P.D. (2003). Analysis of non-adiabatic heat-recirculating combustors. Combustion and Flame 135: 421-439

[4] Maruta K., Kataoka T., Kim N.I., Minaev S., Fursenko R. (2005). Characteristics of combustion in a narrow channel with a temperature gradient. Proceedings of the Combustion Institute 30: 2429-2436

[5] Schoegl I., Ellzey J.L. (2007). Superadiabatic combustion in conducting tubes and heat exchangers of finite length. Combustion and Flame 151: 142-159

[6] Yanenko N. N. (1971). The Method of Fractional Steps, Springer,New York.

[7] Pantakar S. V. (1980). Numerical heat transfer and fluid flow, First Edition, McGraw-Hill, New York.

[8] Kazakov A., Frenklach M. (1994). DRM19 based on GRI-Mech 1.2, http://www.me.berkeley.edu/drm/.